ISSN 2411-3336; e-ISSN 2541-9404

JOURNAL OF MINING INSTITUTE

Zapiski Gornogo instituta

Journal homepage: pmi.spmi.ru

Research article

Geology

New data on the manifestation of Baikalian (Timanian) tectono-magmatic activation on West Spitsbergen Island

Aleksandr N. Sirotkin[1], **Aleksandr N. Evdokimov**[2]✉, **Marina Yu. Burnaeva**[1], **Natalya A. Rumyantseva**[1]

[1] *VNIIOkeangeologia, Saint Petersburg, Russia*

[2] *Empress Catherine II Saint Petersburg Mining University, Saint Petersburg, Russia*

***How to cite this article*:** Sirotkin A.N., Evdokimov A.N., Burnaeva M.Yu., Rumyantseva N.A. New data on the manifestation of Baikalian (Timanian) tectono-magmatic activation on West Spitsbergen Island. Journal of Mining Institute. 2026. Vol. 279, p. 51-69.

Abstract

The Spitsbergen archipelago is at the junction of the northern segment of the Norwegian-Greenland Basin and the western part of the Arctic Ocean, which makes it a key area for deciphering the formation history and geological structure of the region. Crystalline basement rocks and sedimentary cover units outcrop here, including those that constitute the petroleum-bearing complexes of the shelf. There is a clear need to substantiate the presence of evidence for the Baikalian (Timanian) tectono-magmatic activation within the Earth's crust of the Spitsbergen archipelago, as well as to determine the conditions of its manifestation. To address this objective, a comprehensive description of the Trollheimen volcanogenic formation – whose rocks are known within Oscar II Land – is provided for the first time, based on the authors' own data. We examine geotectonic features, material composition, age, and geodynamic interpretations of the formation settings. The authors identified that the sedimentary-volcanogenic complex described in the mountainous glacial part of Oscar II Land was formed during the Vendian (574-558 Ma) as a result of tectono-magmatic activation of the epi-Grenvillian paraplatform. They provide the petrographic and petro-geochemical profile of the identified metabasalts, metaandesites, and metatuffs. The results of studying the petrochemical features of the Trollheimen volcanogenic formation indicate magma generation at great depths; the rift-related nature of these formations is determined. The authors carry out a correlation with the previously identified sedimentary-volcanogenic complex of the Chamberlaindalen Series in the northern part of Wedel Jarlsberg Land. The presented data confirm the previously proposed arguments for the Vendian-Baikalian, Timanian intraplate activation in the archipelago, as well as the widespread development of these complexes within the cover of the epi-Grenvillian paraplatform of Spitsbergen.

Keywords

Spitsbergen archipelago; Oscar II Land; sedimentary-volcanogenic complex; Trollheimen Formation; mafic volcanism; metavolcanic rocks; Vendian; zircon; absolute age; tectono-magmatic activation

Funding

None.

Received: 30.05.2025 ***Accepted: 04.03.2026*** ***Online: 15.05.2026*** ***Published: 20.07.2026***

Introduction

The relevance of this study stems from the need to substantiate the existence of evidence for the Baikalian (Timanian) tectono-magmatic activation [1-3] within the Earth's crust of the Spitsbergen archipelago and the conditions of its manifestation [4, 5]. Relatively recently, a sedimentary-volcanogenic complex of Vendian age was identified in Wedel Jarlsberg Land (WJL), described as the Chamberlaindalen Series [6]. Analysis of the rock composition and their absolute age, as well as other features of this complex, indicates a rift-related nature of its formation at the peak of tectono-magmatic activation of the ancient epi-Grenvillian paraplatform. However, a question arises regarding the scale of this event and its manifestation in other areas of the archipelago. This study presents unique data on another sedimentary-volcanogenic complex of Vendian age, identified by the authors

This is an open access article under the CC BY 4.0 license

within Oscar II Land on the western coast of Spitsbergen. This discovery not only supplements existing knowledge about tectonomagmatic processes in the region but may also significantly expand the understanding of geodynamic processes that occurred in this area in the past. Thus, the work is of considerable importance for further study of the geological history of the archipelago and its tectonic evolution.

Geological framework of the study area

According to current understanding, two main structural levels separated by a structural unconformity are distinguished in the basement of the Barents Plate in the Spitsbergen Anticline area: the Lower Proterozoic – Middle Riphean crystalline basement and the Upper Riphean – Lower Paleozoic ancient platform cover (paraplatform), which underwent later dislocations, magmatism, and partial metamorphism during the Baikalian – Timanian, as well as during the Devonian continental rifting [7, 8].

The crystalline basement of the archipelago is composed of rocks from three lithostructural complexes [5]. The lower complex (PR_1) is represented by a sedimentary-volcanogenic sequence, the regional metamorphism of which dates back to 1750 Ma. The middle complex (RF_1) is characterised by amagmatic features and was formed in a passive continental margin setting. Zonal metamorphism reaching amphibolite facies conditions is dated to the Middle Riphean. The upper complex (RF_2), rift-related in nature, has a sedimentary-volcanogenic character. Low-temperature alterations are associated with burial metamorphism, while the repeated progressive metamorphism of some blocks is linked to the Baikalian and Caledonian tectono-magmatic activation events.

The ancient platform cover (RF_3-PZ_1) is represented by characterised by fossil assemblages successions formed under “platformoid” conditions [1, 3] and in fact constitutes the cover of the epi-Grenvillian paraplatform. Minimal metamorphism is typical for the lower parts of the complex. In the WJL area, sedimentary-volcanogenic formations of the Chamberlaindalen Series (V_2) are identified within this cover; these formations are the result of the Baikalian (Timanian) tectono-magmatic activation [6]. A thick Devonian graben complex (D_{1-2}), known in the central part of the archipelago, owes its origin to the Caledonian rifting [9].

The study area (southern part of Oscar II Land) is within the western coast of Spitsbergen (WCS), which has a highly complex structure (Fig.1) due to the strong impact of Alpine orogeny. The Middle Riphean volcanogenic complex is represented here by thick (over 3000 m) Werenskioldbreen volcanogenic-sedimentary series [10]. In the stratotype section, described in WJL, the series consists of actinolite and chlorite-mica schists with quartzite interlayers; quartzite-sandstones with interlayers of chlorite and mica schists; felsic volcanics. In sections from other areas of the WCS, well-preserved horizons of metabasalts and muscovite-plagioclase-quartz rocks with relicts of porphyritic structures were recorded; these represent felsic meta-effusive rocks [11]. The lower contact of the series is tectonic; the upper boundary is described as a structural unconformity with the overlying rocks of the Upper Riphean Sofiebogen Series [12]. Intrusive formations in WJL are represented by gabbro-granite and peridotite-gabbro bodies. The following ages were obtained for these rocks: for intrusive rocks (U-Pb, Rb-Sr) 1278-1072 Ma; for volcanics of the Werenskioldbreen Series (U-Pb) 1201-919 Ma [13]. New data for the northern part of WJL yield a U-Pb age of 1152-936 Ma for mafic and felsic intrusive rocks [6]. Identical petrological profile and geological setting were described for the Middle Riphean sedimentary-volcanogenic complex in the eastern part of the archipelago [14]. Therefore, we can assert that the structural unconformity between the Middle and Upper Riphean complexes in Spitsbergen is regional and marks the contact between the top of the ancient crystalline basement and the base of the epi-Grenvillian paraplatform.

Within the recently identified sedimentary-volcanogenic sequence of the Chamberlaindalen Series (V_2) in WJL (Fig.1), horizons of weakly metamorphosed basalts, andesite-basalts, andesites and their tuffs with interlayers of phyllites, quartzites, and limestones are widely represented. The contacts with adjacent complexes are tectonic. These volcanic rocks are characterised by U-Pb zircon ages of

This is an open access article under the CC BY 4.0 license

593-559 Ma [6]. The nature of the volcanic rocks and the predominantly pelitic composition of the metasedimentary rocks indicate that the sedimentary-volcanogenic sequence formed during a single tectono-magmatic cycle. During this cycle, moderately alkaline mafic volcanism was combined with a high degree of chemical weathering of rocks in the source areas of the Vendian sediment supply. This allows us to conclude that the depositional settings of the sedimentary-volcanogenic sequence were close in nature to continental rifting.

Thus, in Spitsbergen, two stages of intraplate volcanism are identified for the Late Proterozoic: Middle Riphean – Grenvillian, which concluded the formation of the ancient crystalline basement, and Vendian – Baikalian, Timanian, which occurred in a setting of intraplate tectono-magmatic activation superimposed on the ancient paraplatform structures.

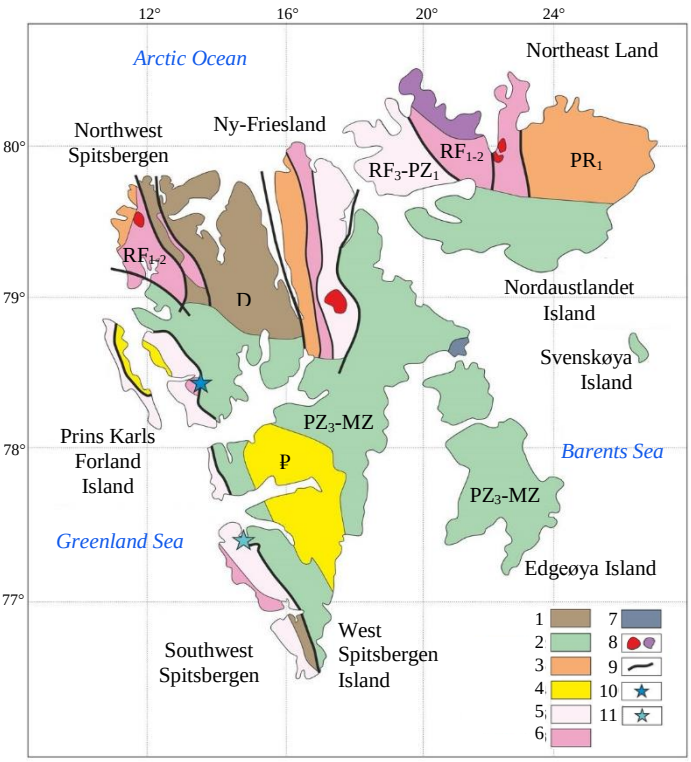


Fig.1. Geological structure of the Spitsbergen archipelago according to [5]

1 – Devonian terrigenous complex; 2 – sedimentary cover complex (PZ_3-MZ); 3 – metamorphic basement complexes (PR_1); 4 – sedimentary cover complex (P); 5 – terrigenous-carbonate paraplatform complexes (RF_3-PZ_1); 6 – metaterrigenous and sedimentary-volcanic basement complexes (RF_{1-2}) with Grenvillian granitoids; 7 – Mesozoic dolerites; 8 – Caledonian granite intrusions; 9 – faults; 10 – study area in the southern part of Oscar II Land and the area of the Vendian metavolcanic outcrops; 11 – area of the Vendian metavolcanic outcrops in the north of Wedel Jarlsberg Land according to [6]

In 2021-2023, during geological surveying in the southern part of Oscar II Land, the authors described outcrops of a sedimentary-volcanogenic sequence in the heads of the Eidembreen and Esmarkbreen glaciers. Previous researchers identified these rocks as independent stratigraphic units, whose age was not determined and was assigned by different authors – by analogy with similar complexes of the archipelago – as ranging from Early to Late Riphean [15, 16]. Work carried out in the 1960-1970s identified a sedimentary-volcanogenic sequence here, dated as the Middle-Late Riphean. The sequence was stratified into two parts: a lower carbonate-terrigenous-volcanogenic unit and an upper terrigenous unit [17-19], both united into the St. Jonsfjorden Group. Later, W.B.Harland [20] revised the age interpretation of the St. Jonsfjorden Group rocks and proposed a Vendian age, uniting them with the Comfortlessbreen Group into a single Vendian straton.

In 2003, Norwegian geologists, while compiling the 1:100,000 geological map for this area, identified the rocks of the complex as the Trollheimen and Løvliebreen formations [21] and united them into the St. Jonsfjorden Group together with the carbonate-terrigenous sequence – the Daudmanns and Alkhornet formations. However, the Norwegians define the age of this complex as Mesoproterozoic.

Thus, the main objective of the present study is to determine the composition and age of the sedimentary-volcanogenic complex of the Trollheimen Fm., which is exposed on nunataks in the southern part of Oscar II Land and has tectonic contacts with the Riphean-Vendian deposits. The rocks of the formation consist of weakly metamorphosed mafic volcanics. Geological contacts with underlying and overlying rocks are not observed, leading to ambiguous assessments of their structural position. The new authors' chart is presented in Fig.2.

This is an open access article under the CC BY 4.0 license

Journal of Mining Institute. *2026. Vol. 279. P. 51-69*
© Aleksandr N. Sirotkin, Aleksandr N. Evdokimov, Marina Yu. Burnaeva, Natalya A. Rumyantseva, 2026

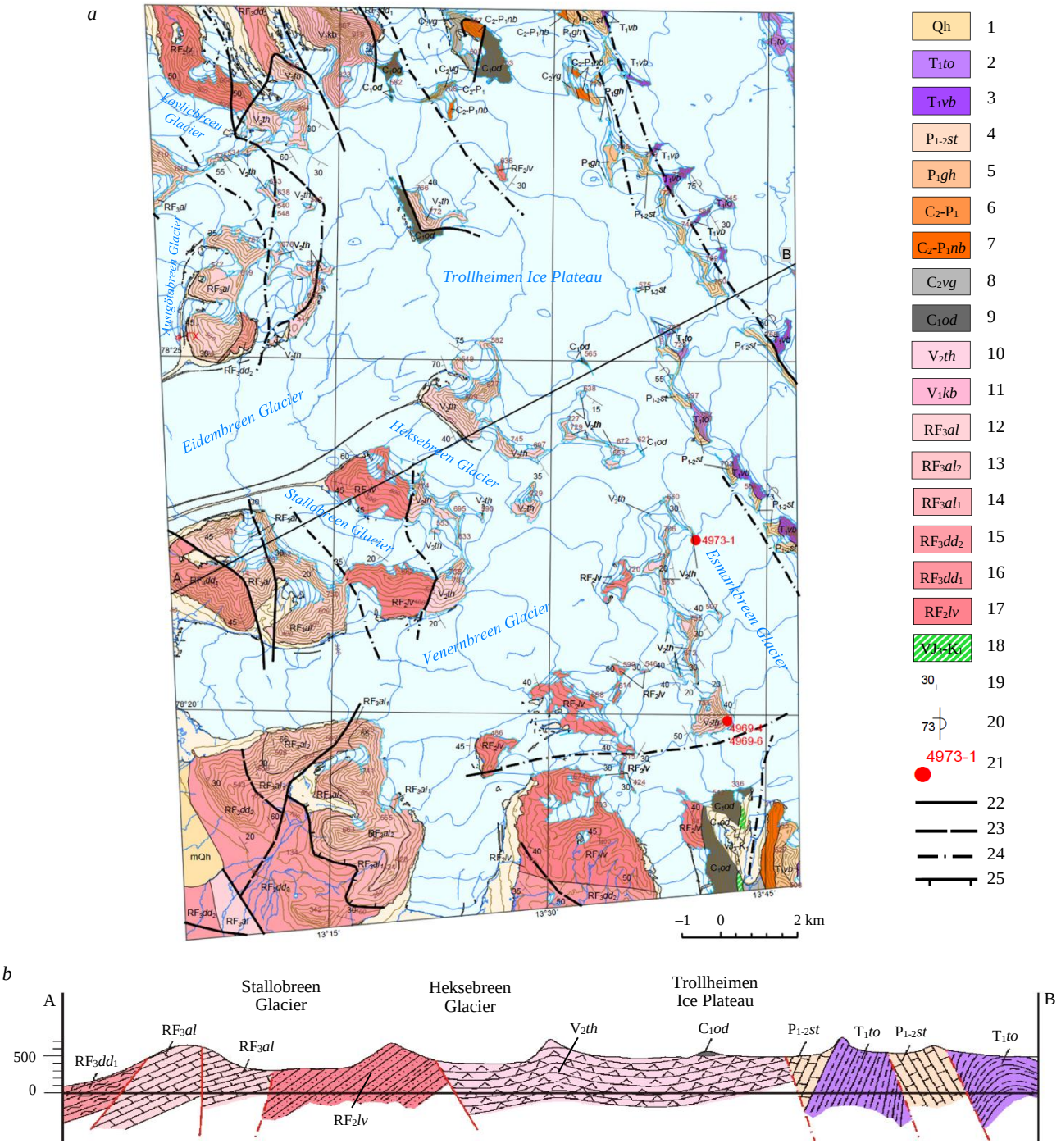


Fig.2. Geological map (*a*) and cross-section (*b*) of the southern part of Oscar II Land, scale 1:100,000, compiled by A.N.Sirotkin

1 – moraine deposits: boulder loams, pebbles, sands and sediments of the modern beach; 2 – Tvillingodden Fm.: siltstones, mudstones; interlayers of limestone, dolomite; calcareous and calcareous-dolomite concretions; 3 – Vardebukta Fm.: sandstones, siltstones, mudstones, interlayers of limestone; phosphorite, calcareous, dolomite, and pyrite concretions; 4 – Tempelfjorden Series, Kapp-Starostin Fm.: dark grey silicites, dolomites, and siliceous siltstones, organogenic-clastic limestone at the base; 5 – Gipshuken Fm.: dolomites, gypsum, anhydrites; 6 – unstratified deposits of the Vegardfjella and Nordenskjöldbreen formations: massive dolomites with interlayers of organogenic-detrital rocks, variegated calcareous sandstones, quartz conglomerates; 7 – Nordenskjöldbreen Fm.: organogenic-detrital limestones with flint nodules and gypsum lenses; 8 – Vegardfjella Fm.: sandstones, variegated siltstones; interlayers of gritstones, conglomerates, sandy limestones; 9 – Orustdalen Fm.: massive grey-coloured sandstones with lenses of quartzite conglomerates, carbonaceous mudstones; 10 – Trollheimen Fm.: mafic and intermediate metavolcanics, greenstone rocks, interlayers of quartzites and sericite-chlorite schists; 11 – unstratified shales of the Haakon and Annabreen formations: shales with “floating” pebbles, quartzites, gritstone lenses; 12-14 – Alkhornet Fm.: 12 – unstratified: limestones, dolomites, clayey-carbonate and carbonate shales, 13 – upper subformation: limestones, dolomites, marbles, clayey-carbonate shales, 14 – lower subformation: limestones, dolomites, clayey-carbonate shales and quartz-micaceous schists; 15, 16 – Daudmanns Fm.: 15 – upper subformation: quartzite-sandstones, quartz-micaceous schists, 16 – lower subformation: limestones, dolomites, quartz-micaceous schists, quartzites; 17 – Løvliebreen Fm.: metapelites, quartzites, metavolcanics; 18 – Mesozoic dolerite complex; 19, 20 – bedding elements and dip angle: 19 – inclined, 20 – overturned; 21 – observation point and its number; 22-25 – tectonic faults: 22 – reliable faults, 23 – inferred faults, 24 – faults inferred under glaciers, 25 – thrusts

This is an open access article under the CC BY 4.0 license



Fig.3. Nunatak Spiret on the western edge of the Esmarkbreen Glacier, composed of metavolcanic rocks of the Trollheimen Fm. Absolute elevation 731 m

Trollheimen Formation

The Trollheimen Fm. was first mapped in the southern part of Oscar II Land [21] as the lowest part of the Riphean sequence. In various maps by previous researchers, it was marked as the Middle-Upper Riphean. The rocks of the formation create rocky nunataks in the area of the Trollheimen ice field and are exposed along the margins of the Eidembreen and Esmarkbreen glaciers (Fig.3).

The dominant rocks of the Trollheimen Fm. are metavolcanics, typically exhibiting porphyritic textures. Among these, metabasalts, metaandesites, as well as various metatuffs and metatuff breccias can be distinguished. The rocks display structural and textural diversity and a wide colour range: from dark grey and grey to grey-green and brown. Within the formation's sequence, the rocks form individual layers that alternate and interbed with each other. Thickness of individual layers varies from 1-2 m to tens of metres. Porphyritic textures are most common, while brecciated and aphyric textures are less frequent. Porphyritic phenocrysts are represented by light-coloured carbonate; they are often green (filled with actinolite or chlorite) and black pyroxenes. The size of phenocrysts reaches 1-2 cm, though more commonly 2-3 mm. The rocks underwent metamorphism under greenschist facies conditions, so the groundmass generally has a quartz-carbonate-actinolite-chlorite composition. The rock texture is schistose; rocks with nearly massive texture are rare. Porous texture, observed in outcrops of metavolcanic rocks, is interpreted as primary amygdaloidal texture, formed during the crystallisation of ancient lavas.

Among the metavolcanic rocks, interlayers of terrigenous rocks occur, represented by metasandstones, metasiltstones, and metatuffites. These are usually dark grey and grey, although brownish varieties are also observed. The contacts with metavolcanic rocks are conformable but sharp. Thickness of individual layers does not exceed 4-5 m. The visible thickness of the formation's rocks in the nunataks amount to hundreds of metres; however, since the base of the formation is unknown, its total thickness can be estimated at over 1000 m.

Løvliebreen Formation

The Løvliebreen Fm. was identified by W.B.Harland [19] on the southern coast of St. Jonsfjorden. No contact with the rocks of the Trollheimen Fm. was observed. The Løvliebreen Fm. is represented by siltstones, quartzites, and gritstones; individual layers of metavolcanic rocks may also be present. The formation thickness reaches 500-600 m. Rock outcrops of the formation are recorded in the western and eastern parts of the Trollheimen ice field. The rock units of the Trollheimen and Løvliebreen formations are separated from surrounding complexes by major faults: in the west – by faults in the middle section of the Eidembreen Glacier; in the east – by a fault along the Esmarkbreen Glacier.

This is an open access article under the CC BY 4.0 license

The rocks of the St. Jonsfjorden Series outcrop to the west of the described structure and are represented by two formations. The lower Daudmanns Fm. was first identified by S.I.Turchenko [22] in Oscar II Land; its stratotype is described in the area of the eponymous plain. Here, the formation is stratified into two units: a lower carbonate-shale unit and an upper quartzite-schist unit, with a total thickness of 3.0-3.5 km. The lower contact of the formation is unknown. The upper Alkhornet Fm. was identified by W.B.Harland [19] and conformably overlies the Daudmanns Fm. deposits. In terms of composition, the formation is divided into two subformations: a lower shale-carbonate subformation and an upper carbonate subformation. The thickness of the formation in the stratotype is 550 m. Overlying Vendian rocks unconformably overlie the formation. Oncolite assemblages of Late Riphean-Vendian age are present in the rocks of the Daudmanns and Alkhorn formations. These correlate with oncoolites in the Upper Riphean Lomfjorden Series of Ny-Friesland Peninsula [23], indicating their Late Riphean age.

The Comfortlessbreen Vendian Series caps the Precambrian sequence. The rocks of the series are mainly mica-carbonate schists. Their key feature is the presence of "floating" pebbles – isolated or sparse inclusions of xenogenic material in the form of flattened or elongated pebbles ranging in size from 2-3 mm to 25-30 cm. The pebbles have a carbonate, less commonly a quartz-carbonate-mica composition. Mica-carbonate schists contain microfossils, which allow these deposits to be dated as the Vendian [22]. In the literature, the rocks of the series are interpreted as metatillites (Vendian glacial deposits). In addition, quartzite interlayers are noted within the sequence. The thickness of the series reaches 600 m.

Methods

We studied metamagmatic and metasedimentary rocks of the Trollheimen Fm. Geochronological samples weighing approximately 3-4 kg each were collected from these rocks. After crushing and sieving the samples, heavy non-magnetic fractions containing zircon were separated using electromagnetic separation and heavy liquids. Zircon monofraction selection was carried out at the Central Analytical Laboratory (CAL) of VSEGEI and the laboratory of Kazan Federal University (KFU). Analyses of their isotopic composition were performed at the Centre of Isotopic Research (CIR) of VSEGEI. The age of zircon was determined by the local U-Pb method using a SHRIMP II ion microprobe, following the standard procedure [24]. Optical (in transmitted and reflected light) and cathodoluminescent (CL) images of zircon were used to select dating points within zircon grains. Rock-forming elements were determined at the laboratory of VNIIOkeangeologia using wet chemistry methods. Trace elements were obtained at the CAL of VSEGEI based on ICP-MS analysis results (Table 1). When constructing REE distribution spectra, their concentrations were normalised to the contents: in CI chondrite, in primitive mantle, and in N-MORB basalts [25]. The study uses rock-forming mineral symbols according to [26].

Table 1

Compositions of metavolcanic rocks of the Trollheimen Fm., wt.%

Components	4765-1	4765-2	4765-3	4765-4	4766-1	4815-1	4815-2
	Chl-Act schist	Porphyritic alkaline metapicrite	Chl-Act schist	Qz-Carb-Chl metapicrite	Chl-Act schist	Metatuff	Metadolerite
SiO_2	45.51	31.72	45.03	36.80	45.59	42.33	46.81
TiO_2	3.49	3.82	3.33	2.64	3.43	4.17	2.93
Al_2O_3	12.68	10.11	12.38	10.31	12.58	13.06	14.21
Fe_2O_3	4.08	9.61	4.29	6.99	4.34	11.63	3.98
FeO	8.96	2.73	8.46	2.08	8.82	3.31	7.28
MnO	0.19	0.13	0.20	0.15	0.20	0.15	0.15
MgO	7.93	4.05	8.46	2.25	8.61	4.07	6.86
CaO	7.17	16.53	7.41	17.52	7.33	7.77	9.02
Na_2O	3.22	0.53	3.11	3.45	3.29	5.25	4.36

This is an open access article under the CC BY 4.0 license

Table 1 continued

Components	4765-1	4765-2	4765-3	4765-4	4766-1	4815-1	4815-2
	Chl-Act schist	Porphyritic alkaline meta-picrite	Chl-Act schist	Qz-Carb-Chl metapicrite	Chl-Act schist	Metatuff	Metadolerite
K_2O	0.63	4.45	0.66	2.51	0.61	1.34	0.34
P_2O_5	0.93	0.33	0.87	0.75	0.73	0.84	0.69
LOI	4.78	15.90	5.34	14.11	4.52	6.15	3.37
Total	99.56	99.92	99.54	99.57	100.00	100.10	100.00
CO_2	1.40	12.58	1.84	11.88	1.02	n.d.	n.d.
Sc	20.3	14.5	20.7	13.5	19.7	17.6	26.1
Co	43.6	42	41.8	27.8	43.5	27.3	28.2
Ni	121	181	113	65	118	113	98.8
Cu	45.7	2.89	49.5	31.9	47.7	98.9	17.8
V	218	112	229	184	223	226	236
Cr	229	423	217	130	232	174	160
Ga	20.3	19.4	20	14.2	20.5	23.1	21.2
Rb	7.02	79.1	6.94	29.5	6.37	12.3	2.54
Sr	441	604	480	636	471	449	2500
Y	26.6	19.7	27.8	21.4	28	42.6	26.7
Zr	245	289	243	225	256	405	208
Nb	45.7	52	42.8	41.2	48.7	71.7	38.4
Ba	160	600	126	745	147	306	329
La	44.7	39.5	43.7	42.1	46.7	69.7	34.7
Ce	98.6	90.4	97.3	86.6	104	145	73.7
Pr	13.8	13.2	13.2	11.7	14	20.1	9.5
Nd	57.7	55.4	57.9	45.3	60.6	91.5	42.3
Sm	11.9	10.2	11.7	8.15	12	18.8	10
Eu	3.48	2.83	3.42	2.81	3.93	5.82	2.84
Gd	9.42	7.97	9.29	7.04	9.41	15.3	8.31
Tb	1.22	1.03	1.3	0.97	1.22	2.01	1.14
Dy	6.16	4.77	6.22	4.93	6.67	9.63	5.8
Ho	1.05	0.88	1.13	0.87	1.24	1.71	1.02
Er	2.51	2	2.68	2.13	2.92	4.13	2.47
Tm	0.36	0.29	0.41	0.23	0.35	0.48	0.32
Yb	2.1	1.73	2.11	1.6	2.05	2.96	1.84
Lu	0.24	0.17	0.29	0.21	0.24	0.42	0.24
Hf	6.62	7.23	6.55	5.98	6.83	10.8	5.36
Th	2.42	2.73	2.45	2.84	2.68	5.33	2.88

Components	4818-1	4818-2	4818-3	4818-4	4863-1	4864-1	4864-2
	Carb-Chl shale	Qz-Ms-Chl schist	Metapicrite	Metatuff	Ms-Chl metapicro-basalt	Porphyry Chl-Act metabasalt	Metaandesite
SiO_2	31.97	42.24	32.34	49.90	41.16	43.99	49.28
TiO_2	2.73	8.07	5.46	2.85	4.39	3.96	2.70
Al_2O_3	10.43	12.04	14.23	10.30	13.31	10.72	12.93
Fe_2O_3	8.61	10.43	0.61	11.75	9.24	5.93	4.37
FeO	2.85	3.64	16.23	2.72	3.18	5.48	6.79
MnO	0.19	0.11	0.13	0.07	0.13	0.13	0.15
MgO	4.33	9.21	14.56	9.21	6.48	6.66	7.59
CaO	17.54	3.07	4.27	3.05	6.95	10.54	7.80
Na_2O	4.78	0.14	0.15	1.56	3.75	3.66	3.20
K_2O	0.52	3.51	0.10	1.09	2.01	1.28	0.90
P_2O_5	0.89	0.90	1.15	0.38	1.21	0.54	0.29
LOI	14.96	6.98	10.90	6.88	7.93	6.91	3.67
Total	99.79	100.00	100.10	99.75	99.73	99.80	99.66
CO_2	n.d.	n.d.	n.d.	n.d.	n.d.	n.d.	n.d.
Sc	16.9	39.2	22.5	17.9	24.4	30.3	39.5
Co	32.8	90.6	46.7	42.4	28.9	34.1	37
Ni	109	199	295	227	95.1	213	148
Cu	8.08	20.1	121	57.2	38.8	54.3	32.5
V	235	389	371	219	214	248	200
Cr	171	424	315	286	173	367	303
Ga	17.3	24.2	22.9	14.7	17.6	16.5	18.1

This is an open access article under the CC BY 4.0 license

© Aleksandr N. Sirotkin, Aleksandr N. Evdokimov, Marina Yu. Burnaeva, Natalya A. Rumyantseva, 2026

Table 1 continued

Components	4818-1	4818-2	4818-3	4818-4	4863-1	4864-1	4864-2
	Carb-Chl shale	Qz-Ms-Chl schist	Metapicrite	Metatuff	Ms-Chl metapicro-basalt	Porphyry Chl-Act metabasalt	Metaandesite
Rb	8.19	60.4	2	10.6	14.9	10.3	13.1
Sr	512	167	154	110	267	232	874
Y	24.9	24.2	28.6	17	25.6	26	26.2
Zr	216	328	323	176	285	235	152
Nb	36.3	47.9	55.5	30.4	39	18.7	13.1
Ba	135	383	54.3	189	296	317	288
La	32.9	27.4	46.1	22.3	33.4	19.9	13.7
Ce	75.5	72.9	112	48.8	80.2	51.9	29.5
Pr	10.2	10.3	15.4	6.39	11.6	7.99	4.02
Nd	46.1	47.9	68.5	28	50.7	38.5	18.9
Sm	10	10.3	14.3	6.09	10.3	8.97	4.85
Eu	2.9	3.01	3.66	1.82	3.06	2.85	1.77
Gd	8.22	8.74	11.1	4.85	9.52	7.95	5.89
Tb	1.04	1.13	1.29	0.67	1.19	1.07	0.92
Dy	5.47	5.63	6.68	3.64	6.16	5.65	5.27
Ho	1.02	1.01	1.19	0.72	1.1	1.02	1.09
Er	2.55	2.5	2.76	1.86	2.46	2.43	2.55
Tm	0.31	0.3	0.43	0.16	0.33	0.29	0.35
Yb	1.98	1.64	2.2	1.3	1.87	1.95	1.93
Lu	0.25	0.21	0.33	0.17	0.25	0.24	0.28
Hf	5.83	10.7	9	4.88	7.42	6.22	4.08
Th	2.1	1.36	3.97	1.89	2.44	1.09	1.95

Components	4865-1	4865-2	4914-1	4914-2	4914-3	4914-5	4969-1
	Metapicro-basalt	Amygdaloidal picrobasalt	Carb-Chl shale	Carb-Chl shale	Carbonated metapicrite	Amygdaloidal metapicrite	Carbonated metapicrite
SiO_2	44.59	41.22	37.91	38.18	34.71	32.72	32.35
TiO_2	4.26	2.48	4.44	4.26	2.95	3.31	2.37
Al_2O_3	13.80	10.93	12.71	9.86	4.37	8.23	5.38
Fe_2O_3	3.59	1.63	4.76	9.35	2.42	4.65	3.13
FeO	7.94	6.94	6.52	3.68	2.02	7.10	5.02
MnO	0.09	0.24	0.16	0.15	0.22	0.29	0.21
MgO	9.29	7.36	9.58	8.55	4.60	7.00	2.63
CaO	3.75	11.08	7.58	9.79	25.53	15.54	24.98
Na_2O	3.26	2.52	2.15	2.08	0.25	1.19	0.13
K_2O	0.84	0.61	0.30	0.99	0.61	0.65	0.99
P_2O_5	1.42	0.99	0.87	0.52	0.87	0.67	0.85
LOI	6.78	13.75	12.94	12.33	21.34	18.46	21.92
Total	99.60	99.78	99.93	99.74	99.89	99.78	99.97
CO_2	n.d.	n.d.	8.11	9.30	20.08	15.58	19.27
Sc	14	11.5	18.3	30.6	23.7	28.9	21.6
Co	29	21.7	32.4	60.0	30.6	47.7	48.0
Ni	38.8	92.4	99.3	233.9	151.2	159	105.6
Cu	33.8	24.9	42.5	40.1	336.6	54.3	68.8
V	239	150	124	182	97.2	222	66.3
Cr	44.8	197	218	475.7	489	354.7	191
Ga	25.1	17	15.9	25.2	15.1	25.2	24.6
Rb	10.5	6.35	11.0	17.3	16.3	15.9	22.0
Sr	293	711	1153	291.9	795	643	836
Y	37.5	26.3	20.1	22.4	17.3	24.3	36.5
Zr	478	471	99.1	190.1	133.6	154.6	218.9
Nb	93.1	34.7	22.4	49.2	34.0	39.7	47.7
Ba	189	186	267	338.7	1375	315.5	287.5
La	70.4	43.4	24.3	29.1	21.5	33.7	53.9
Ce	158	107	57.8	70.2	51.2	82.6	103.6
Pr	21.2	15.7	7.90	9.4	7.0	10.6	13.4
Nd	86.9	69.5	40.8	45.2	33.8	51.0	64.0
Sm	17.7	12.1	8.53	8.52	6.7	10.2	12.0
Eu	4.53	3.38	2.73	2.44	2.1	2.8	3.31
Gd	14.7	10.1	6.66	7.08	5.3	8.0	9.66

This is an open access article under the CC BY 4.0 license

Table 1 continued

Components	4865-1	4865-2	4914-1	4914-2	4914-3	4914-5	4969-1
	Metapicro-basalt	Amygdaloidal picrobasalt	Carb-Chl shale	Carb-Chl shale	Carbonated metapicrite	Amygdaloidal metapicrite	Carbonated metapicrite
Tb	1.72	1.29	0.80	0.94	0.64	0.99	1.17
Dy	8.85	5.94	3.72	4.61	3.18	4.83	6.04
Ho	1.48	1.11	0.62	0.79	0.56	0.82	1.06
Er	3.63	2.36	1.42	1.87	1.39	2.01	2.67
Tm	0.50	0.30	0.18	0.23	0.17	0.24	0.33
Yb	2.83	1.84	1.01	1.27	1.02	1.44	2.02
Lu	0.38	0.24	0.14	0.16	0.13	0.18	0.28
Hf	11.7	11.5	2.10	4.48	3.02	3.33	4.08
Th	5.22	2.11	1.12	1.88	1.48	1.69	2.46

Components	4969-2	4969-3	4969-4	4969-6	4970-1	4970-3	4971-2
	Chl-Carb picrite	Carb-Chl shale	Porphyritic metapicrite	Porphyritic metapicrite	Carb-Chl shale	Qz-Carb-Chl metapicrite	Metapicro-basalt
SiO_2	20.01	39.35	31.54	36.35	31.65	40.45	41.85
TiO_2	2.45	3.52	4.19	2.77	3.20	3.64	6.45
Al_2O_3	5.48	10.55	10.38	10.55	9.61	11.16	11.16
Fe_2O_3	2.43	8.50	2.26	2.53	7.69	3.45	7.44
FeO	6.54	2.56	8.25	8.70	4.30	9.82	8.16
MnO	0.12	0.18	0.15	0.22	0.14	0.10	0.14
MgO	2.70	4.61	6.61	7.18	7.29	9.40	12.18
CaO	31.53	13.47	16.18	14.81	17.72	8.08	2.17
Na_2O	0.19	3.56	0.25	0.63	0.13	0.08	0.21
K_2O	0.44	1.60	1.86	0.23	0.23	0.76	1.72
P_2O_5	0.54	0.90	1.96	1.20	0.32	0.51	0.75
LOI	27.24	10.88	16.27	14.56	17.49	12.59	7.50
Total	99.68	99.69	99.92	99.75	99.77	100.00	99.74
CO_2	25.05	9.05	11.51	10.00	13.60	6.27	1.34
Sc	18.5	26.3	26.2	22.6	29.1	34.8	44.3
Co	29.9	42.3	35.0	48.9	55.8	70.5	71.8
Ni	92.5	227.2	50.6	84.3	222	284	116
Cu	7.74	6.52	8.69	0.11	10.1	13.3	0.11
V	131.2	213.9	249	199	231	157	465
Cr	190.8	522	126.9	156.6	475	525	333
Ga	22.3	29.3	39.0	35.2	25.6	30.6	35.1
Rb	9.14	13.0	27.0	18.7	35.0	9.68	35.6
Sr	890	752	749	531	553	181	173
Y	21.7	26.0	37.0	29.7	20.4	25.3	25.1
Zr	216	392	495	410	254	322	405
Nb	48.4	73.2	88.8	68.5	59.2	65.9	66.4
Ba	128.2	627	622	426	640	189	514
La	34.8	47.3	64.9	56.7	30.1	41.2	34.2
Ce	78.3	103.9	145.1	127.7	70.1	92.8	82.4
Pr	10.0	13.1	19.7	15.5	8.88	11.5	10.9
Nd	47.8	59.0	91.8	69.5	38.8	52.2	53.2
Sm	9.19	10.7	16.4	11.7	7.33	9.52	10.5
Eu	2.30	3.05	4.4	3.14	2.11	2.90	2.96
Gd	6.80	7.94	12.1	8.43	5.80	7.24	7.99
Tb	0.85	1.01	1.42	1.05	0.78	1.0	0.99
Dy	4.23	4.98	7.05	5.39	4.15	5.17	4.94
Ho	0.73	0.88	1.21	0.93	0.72	0.92	0.84
Er	1.79	2.14	2.94	2.32	1.76	2.24	2.09
Tm	0.22	0.26	0.35	0.29	0.21	0.27	0.25
Yb	1.24	1.59	2.1	1.75	1.30	1.61	1.48
Lu	0.15	0.20	0.27	0.21	0.16	0.21	0.20
Hf	4.0	7.47	8.75	7.21	4.99	6.44	8.75
Th	2.33	3.12	3.29	2.92	2.48	2.90	1.90

This is an open access article under the CC BY 4.0 license

© Aleksandr N. Sirotkin, Aleksandr N. Evdokimov, Marina Yu. Burnaeva, Natalya A. Rumyantseva, 2026

End of Table 1

Components	4972-2	4973-1	4975-3
	Act-Chl meta-picrobasalt	Metaandesite	Chl-Act metabasalt
SiO_2	43.22	57.43	44.83
TiO_2	3.55	1.93	3.59
Al_2O_3	8.72	10.91	10.23
Fe_2O_3	1.29	2.46	4.74
FeO	8.67	6.43	5.73
MnO	0.14	0.10	0.14
MgO	8.18	4.54	7.28
CaO	10.89	4.79	12.33
Na_2O	0.47	0.28	1.63
K_2O	1.42	2.56	0.97
P_2O_5	0.60	1.96	0.52
LOI	12.95	6.61	7.82
Total	100.10	100.00	99.80
CO_2	7.85	2.64	5.69
Sc	28.8	27.7	38.1
Co	48.9	37.3	50.6
Ni	195	222	298
Cu	0.13	36.0	34.1
V	186	248	272
Cr	386	498	750
Ga	26.6	32.9	21.6
Rb	22.7	48.3	8.28
Sr	558	206	336
Y	25.5	39.4	25.1
Zr	332	169	251
Nb	49.1	30.6	19.7
Ba	708	481	444
La	28.5	68.5	16.6
Ce	70.2	137	43.6
Pr	9.62	16.4	6.40
Nd	47.6	75.8	33.3
Sm	9.34	14.1	7.61
Eu	2.64	4.69	2.43
Gd	7.42	12.0	6.68
Tb	0.92	1.41	0.85
Dy	4.74	6.61	4.50
Ho	0.86	1.12	0.81
Er	2.06	2.65	2.00
Tm	0.25	0.33	0.25
Yb	1.49	2.02	1.43
Lu	0.18	0.27	0.18
Hf	6.45	3.06	5.19
Th	1.89	1.79	0.65

Rock petrography

Metavolcanic rocks are microscopically represented by an association of newly formed metamorphic minerals. Among relict minerals, monoclinic pyroxene is present, represented by Aug (Ti-Aug). This mineral occurs as porphyritic phenocrysts, emphasising the primary magmatic structure of the rocks, and within the groundmass. Phenocrysts can also be composed of Act, Ab, more commonly, calcite. Calcite phenocrysts are observed either as single grains or as aggregates of large grains of this mineral. The groundmass of the rocks is composed of Chl, Act, Carb, Ms, Ab, Ep, Qz, Spn, Cpx, and Kfs (Fig.4). Accessory minerals are represented by Zrn, Rt, Brt, and Ap. The rocks contain abundant ore mineral, sometimes up to 50-60 %, represented by Py, Ilm, Ti-Mag, rarely Ccp. Cal in phenocrysts is generally magnesian, while Cal in the groundmass is, in contrast, enriched in Sr and Mn. Ab corresponds to plagioclase number 0-1 in composition. Occasionally, Ab in the groundmass is slightly enriched in K or Fe. Light mica may be represented by Ms or, rarely, Pg. Mineral proportions in the rocks vary depending on their petrochemical composition, but overall, the metamorphic paragenesis is represented by Act + Chl + Ms + Ep + Ab + Carb + Opq, corresponding to metamorphism under greenschist facies conditions. The presence of primary magmatic minerals such as Ti-Aug and Kfs indicates elevated alkalinity of these volcanic rocks*. Metasedimentary rocks (siltstones, sandstones) of the Trollheimen Fm. are characterised by the Q + Chl + Ms + Carb + Opq paragenesis, which also corresponds to the greenschist facies.

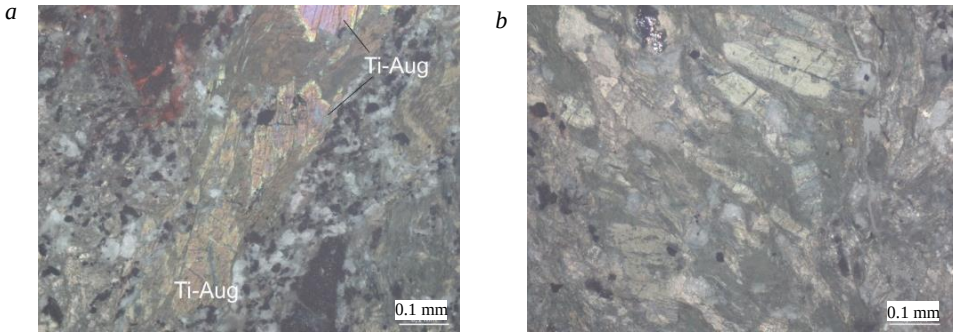


Fig.4. Thin section 4864-1 (+): relics of porphyritic Ti-Aug phenocrysts in metavolcanic rocks (left) (*a*); thin section 4975-3 (+): Carb – Act – Chl matrix of metavolcanic rocks (*b*)

* Petrographic Code of Russia. Igneous, metamorphic, metasomatic, and impact formations. Ed. by O.A.Bogatikov, O.V.Petrov. St. Petersburg: VSEGEI Press, 2009, p. 200.

This is an open access article under the CC BY 4.0 license

Petrochemistry

Chemical composition of metavolcanic rocks is presented in Table 1. In terms of major element content, the studied rocks are mafic and ultramafic, rarely intermediate ones. They are characterised by the following variations in petrogenic elements, wt.%: SiO_2 31.54-57.43; TiO_2 1.93-8.07; Al_2O_3 4.37-14.23; MgO 2.25-14.56; CaO 2.17-31.53; Na_2O 0.08-5.25; K_2O 0.10-4.45. Wide variations in loss on ignition (LOI) are noted – up to 27.24 %, which is related to low-temperature metamorphism of the rocks. In the TAS diagram, the imaging points of the rocks fall mainly into the fields of moderately alkaline and alkaline rocks (trachybasalts, trachypicrites, alkaline basalts, and picrites), and to a lesser extent into the fields of normally alkaline rocks (basalts, picrites). One sample is separated from the others and falls into the andesite field (Fig.5, *a*). The use of normative mineral compositions of metavolcanic rocks (according to the CIPW norm) allowed to supplement the understanding of the types of these basaltoids (Fig.5, *c*). In the diagram, imaging points corresponding to rock compositions are divided into three groups: nepheline (and leucite)-normative alkaline rocks; olivine-pyroxene rocks corresponding to normal basalts; quartz-normative rocks, which may include both metaandesites and metatuffs (metatuffites).

According to alkalinity type, these rocks are divided into two groups: high-K and calc-alkaline. On the K_2O – Na_2O diagram (Fig.5, *b*), a clear differentiation of rocks by alkalinity type is observed, which may indicate different depths of the parental magma origin. In terms of alumina index, the rocks are classified as low-alumina, with only a few samples being moderately aluminous. Based on magnesia content, these are low- and medium-magnesian rocks (Mg 0.29-0.53). The titanium index ranges from 19.7 to 66.7, classifying the rocks as high-titanium.

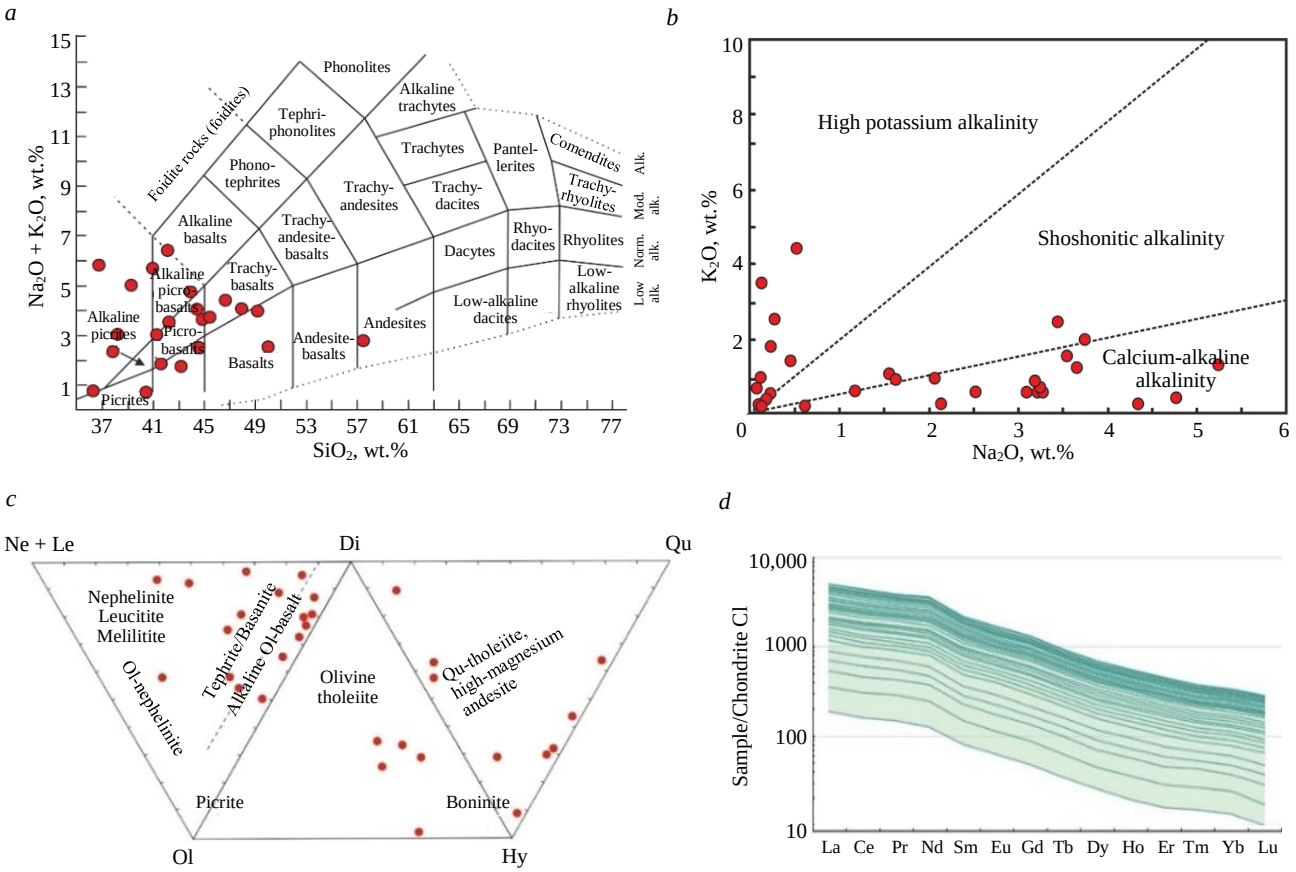


Fig.5. Compositional characteristics of the Trollheimen Fm. metavolcanics:
a – TAS diagram according to the Petrographic Code of Russia; *b* – K_2O – Na_2O diagram according to [27];
c – Qu – Hy – Di – Ol – Ne + Le diagram; *d* – REE distribution spectra normalized to CI chondrite according to [25]

This is an open access article under the CC BY 4.0 license

© Aleksandr N. Sirotkin, Aleksandr N. Evdokimov, Marina Yu. Burnaeva, Natalya A. Rumyantseva, 2026

On variation diagrams SiO_2 – petrogenic elements, the imaging points of the rocks form a single cloud with no signs of differentiation. The exception is the SiO_2 – CaO diagram, which shows a strong inverse relationship, apparently indicating differentiation of rocks by basicity. Variation diagrams MgO – petrogenic elements show a direct correlation with TiO_2, Al_2O_3, and ΣFe; an inverse relationship is observed for CaO. There is no correlation between petrogenic elements and the sum of REE.

REE distribution patterns (Fig.5, *d*) are characterised by a slight smooth slope from light REE to heavy REE and the absence of a pronounced Eu minimum (Eu/Eu* 0.856-1.131). The total REE content varies significantly, ranging from 91.02 to 392.82 g/t: the sum of light REE varies from 72.74 to 358.73 g/t, the sum of heavy REE varies from 16.7 to 34.09 g/t. Element ratios La/Yb 11.6-33.9 and Lu/Gd 0.021-0.031 indicate a significant degree of material fractionation; Nb/La > 1 indicates minimal contamination of the parental magma by crustal material.

On the trace-element spider diagram (normalised to primitive mantle abundances), the studied rocks show an uneven increase in the content of large-ion lithophile elements and high-field-strength elements relative to heavy rare-earth elements. This may indicate the evolution of the magmatic melt under conditions of interaction with a crustal material of elevated alkalinity [27]. Low and decreased contents of compatible elements such as Cr, Ni, Co, etc. may suggest an anatectic nature of mantle melting in the magmatic source and its relative depth.

To reconstruct the geodynamic settings of mafic volcanism, discrimination diagrams proposed by various authors were used (Fig.6). The imaging points corresponding to the metavolcanic rocks of the Trollheimen Fm. fall into the fields of alkaline intraplate basalts and ocean-island basalts. On this basis, these rocks can be interpreted as intraplate magmatites formed during continental rifting.

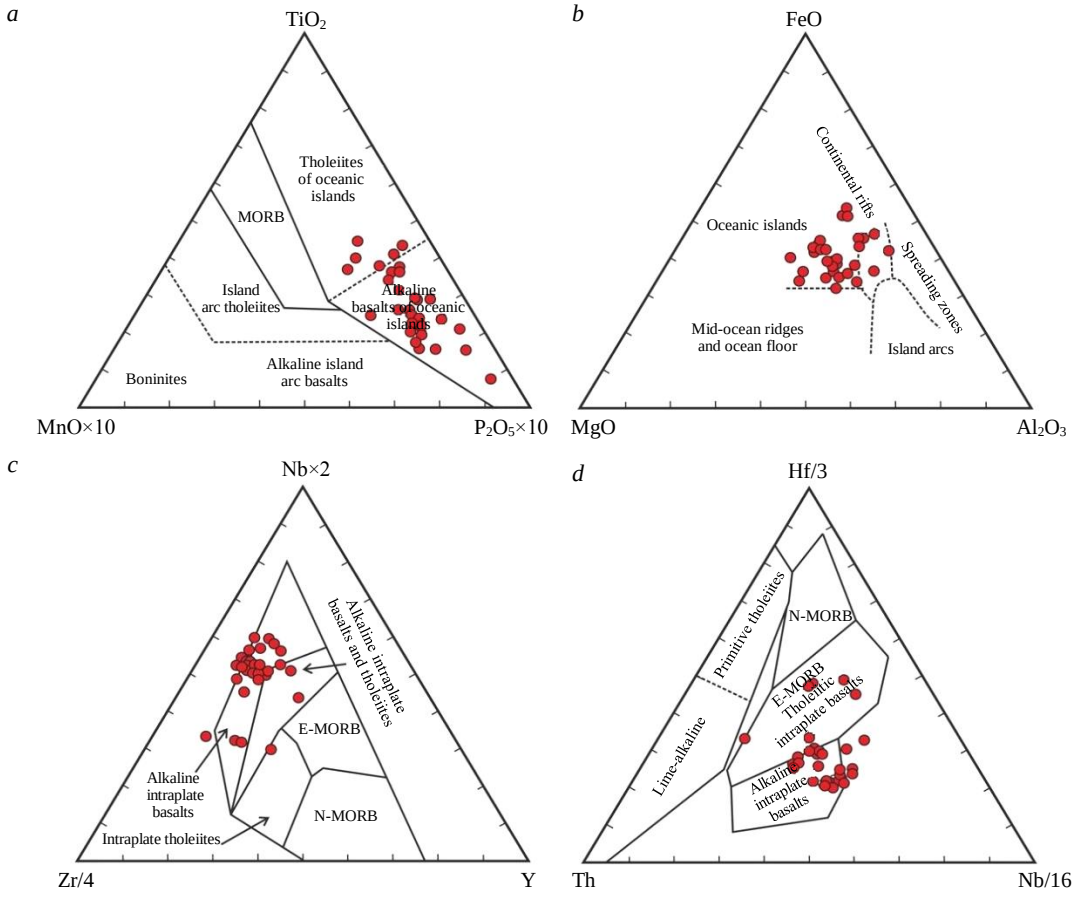


Fig 6. Discrimination diagrams for basaltoids: *a* – TiO_2 – MnO×10 – P_2O_5×10 according to [28]; *b* – FeO – MgO – Al_2O_3 according to [29]; *c* – Nb×2 – Zr/4 – Y according to [30]; *d* – Hf/3 – Th – Nb/16 according to [31]

This is an open access article under the CC BY 4.0 license

Absolute age determination

This study was performed on zircons from rocks of the Trollheimen Fm. Metavolcanics were sampled in the area of nunatak Spiret (samples 4969-4 and 4969-6) and in the upper part of the western slope of the Esmarkbreen Glacier (sample 4973-1) (see Fig.2, 3).

A zircon sample of 30 grains was obtained from greenstone sample 4969-4. The zircon is represented by colourless, light pink, pink, transparent and translucent angular and rounded fragments, as well as fragments of subhedral crystals, some with inclusions and/or fractures. The zircon length ranges from 50 to 122 μm. In the CL images, most zircon grains exhibit a heterogeneous internal structure, expressed by finely banded oscillatory zoning (e.g., grains 1-7, 11-13 in Fig.7, *a*), characterising the magmatic origin of the zircon.

A concordant U-Pb age of 563.2 ± 3.6 Ma (MSWD = 0.17, Fig.7, *b*, Table 2) was recorded for thirteen analysed zircons. The U content at the analysed points varies widely from 56 to 447 ppm (antennary points 11 and 6 in Fig.7, *a*). The Th content varies from 26 to 442 ppm (antennary points 1 and 4 in Fig.7, *a*). The lowest contents of these elements are observed in the lightest areas of zoning in grains in CL images. The Th/U ratio in dated zircon varies from 0.36 to 1.04, averaging 0.69.

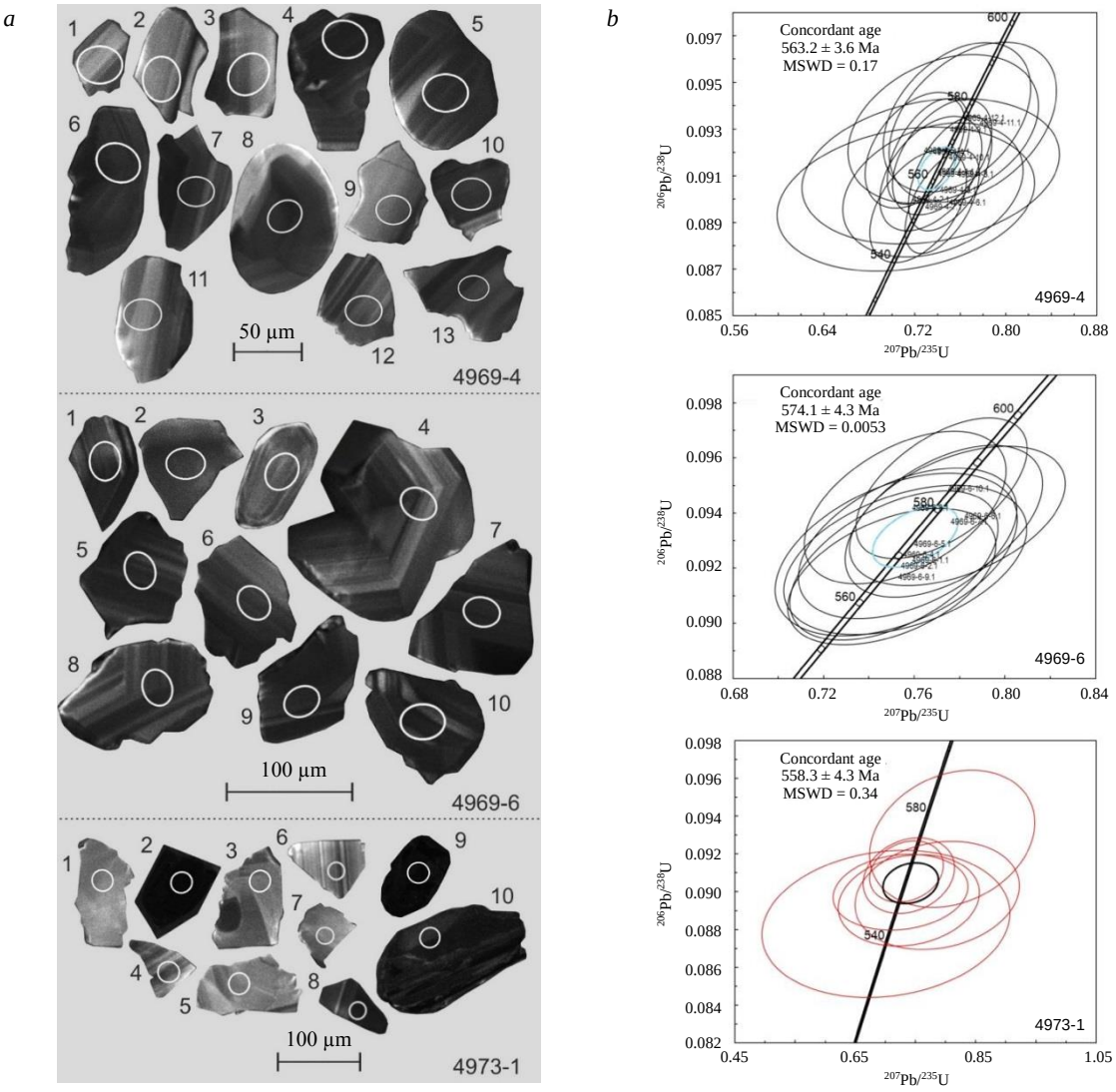


Fig.7. Results of isotope dating of zircon from metavolcanics of the Trollheimen Fm.:
a – grain images in CL images, circles show the position of analytical craters (U-Pb dating); *b* – diagrams with concordia

This is an open access article under the CC BY 4.0 license

This is an open access article under the CC BY 4.0 license

Journal of Mining Institute. 2026. Vol. 279. P. 51-69

© Aleksandr N. Sirotkin, Aleksandr N. Evdokimov, Marina Yu. Burnaeva, Natalya A. Rumyantseva, 2026

Table 2

Results of U-Pb local analysis of zircons from metavolcanics of the Trollheimen Fm. (Oscar II Land, Spitsbergen archipelago)

Analysis point	^{206}Pbc, %	U, ppm	Th, ppm	^{232}Th/^{238}U	^{206}Pb*, ppm	(1) ^{206}Pb/^{238}U Age		(1) ^{207}Pb/^{206}Pb Age		*D*, %	Total ^{238}U/^{206}Pb	±%	Total ^{207}Pb/^{206}Pb	±%	(1) ^{238}U/^{206}Pb*	±%	(1) ^{207}Pb*/^{206}Pb*	±%	(1) ^{207}Pb*/^{235}U	±%	(1) ^{206}Pb*/^{238}U	±%	Rho
Sample 4969-4																							
1	0.63	74	26	0.36	5.84	562.7	±7.8	544	±130	–3	10.89	1.4	0.0636	3	10.96	1.4	0.0584	6.1	0.734	6.3	0.0912	1.4	0.230
2	0.65	74	35	0.49	5.74	555.7	±7.7	504	±140	–9	11.04	1.4	0.0626	3	11.11	1.4	0.0573	6.3	0.712	6.5	0.09	1.4	0.224
3	0.47	116	75	0.67	9.05	557.8	±6.8	571	±91	2	11.01	1.3	0.0629	2.4	11.06	1.3	0.0591	4.2	0.736	4.4	0.0904	1.3	0.293
4	0.12	441	442	1.04	34.9	567.6	±5.6	511	±34	–10	10.85	1	0.0585	1.3	10.87	1	0.05751	1.6	0.73	1.9	0.09204	1	0.551
5	0.22	244	175	0.74	19.3	567.8	±6	485	±53	–15	10.84	1.1	0.0587	1.7	10.86	1.1	0.0568	2.4	0.722	2.6	0.0921	1.1	0.417
6	0.11	447	434	1.00	34.6	554.7	±5.5	605	±33	9	11.12	1	0.06093	1.3	11.13	1	0.06004	1.5	0.744	1.8	0.08987	1	0.558
7	0.17	291	259	0.92	22.4	554	±6	545	±46	–2	11.12	1.1	0.05977	1.6	11.14	1.1	0.0584	2.1	0.723	2.4	0.0897	1.1	0.471
8	0.07	311	248	0.82	24.4	562	±5.8	597	±36	6	10.97	1.1	0.06039	1.5	10.98	1.1	0.05981	1.7	0.751	2	0.09109	1.1	0.541
9	0.31	71	34	0.49	5.66	573.4	±7.8	534	±95	–7	10.72	1.4	0.0606	3.2	10.75	1.4	0.0581	4.4	0.745	4.6	0.093	1.4	0.311
10	0.10	217	171	0.81	17.1	565.9	±6.1	559	±45	–1	10.89	1.1	0.0596	1.8	10.9	1.1	0.0588	2.1	0.744	2.4	0.0918	1.1	0.476
11	0.00	56	29	0.53	4.49	575.2	±8.4	600	±79	4	10.71	1.5	0.0599	3.6	10.71	1.5	0.0599	3.6	0.771	3.9	0.0933	1.5	0.388
12	0.21	107	37	0.36	8.61	576.1	±7.6	556	±71	–4	10.67	1.4	0.0604	2.6	10.7	1.4	0.0587	3.3	0.757	3.5	0.0935	1.4	0.391
13	0.11	208	155	0.77	16.3	562.1	±6.1	547	±48	–3	10.96	1.1	0.0593	1.9	10.98	1.1	0.0585	2.2	0.734	2.5	0.0911	1.1	0.462
Sample 4969-6																							
9	0.12	199	126	0.66	15.7	565.6	± 6.2	580	±48	3	10.89	1.1	0.0603	1.9	10.91	1.1	0.0594	2.2	0.75	2.5	0.0917	1.1	0.458
2	0.00	164	97	0.61	13	567.9	± 6.8	573	±46	1	10.86	1.2	0.0592	2.1	10.86	1.2	0.0592	2.1	0.751	2.5	0.0921	1.2	0.504
1	0.15	151	66	0.46	12	569.3	± 6.6	582	±58	2	10.81	1.2	0.0606	2.3	10.83	1.2	0.0594	2.7	0.756	2.9	0.0923	1.2	0.412
4	0.00	113	65	0.60	8.98	570.6	± 6.9	564	±57	–1	10.8	1.3	0.0589	2.6	10.8	1.3	0.0589	2.6	0.752	2.9	0.0925	1.3	0.437
5	0.12	189	76	0.42	15.1	572.9	± 6.3	571	±50	0	10.75	1.1	0.0601	2	10.76	1.2	0.0591	2.3	0.757	2.6	0.0929	1.2	0.451
7	0.00	187	119	0.66	15	577.4	± 6.4	596	±43	3	10.67	1.2	0.0598	2	10.67	1.2	0.0598	2	0.773	2.3	0.0937	1.2	0.498
6	0.11	200	127	0.66	16.1	578.8	± 6.3	609	±47	5	10.63	1.1	0.0611	1.9	10.65	1.1	0.0602	2.2	0.779	2.5	0.0939	1.1	0.463
8	0.00	173	81	0.49	14	580.2	± 6.5	538	±46	–7	10.62	1.2	0.0582	2.1	10.62	1.2	0.0582	2.1	0.756	2.4	0.0942	1.2	0.484
10	0.00	272	155	0.59	22.2	584.7	± 6.4	567	±37	–3	10.53	1.1	0.059	1.7	10.53	1.1	0.059	1.7	0.772	2	0.0949	1.1	0.559
3	0.00	119	100	0.87	30.4	1675	±18	1647	±21	–2	3.371	1.2	0.1012	1.1	3.371	1.2	0.1012	1.1	4.14	1.7	0.2966	1.2	0.738

End of Table 2

Analysis point	^{206}Pbc, %	U, ppm	Th, ppm	^{232}Th/^{238}U	^{206}Pb*, ppm	(1) ^{206}Pb/^{238}U Age		(1) ^{207}Pb/^{206}Pb Age		*D*, %	Total ^{238}U/^{206}Pb	±%	Total ^{207}Pb/^{206}Pb	±%	(1) ^{238}U/^{206}Pb*	±%	(1) ^{207}Pb*/^{206}Pb*	±%	(1) ^{207}Pb*/^{235}U	±%	(1) ^{206}Pb*/^{238}U	±%	Rho
Sample 4973-1																							
1	1.34	37	18	0.52	2.81	545.4	±9.4	515	±270	–6	11.33	1.8	0.0576	12	0.701	12	0.0883	1.8	0.146	12	0.0883	1.8	0.146
7	0.59	73	55	0.78	5.65	552.8	±5.8	598	±140	8	11.17	1.1	0.0599	6.4	0.739	6.5	0.0895	1.1	0.168	6.5	0.08954	1.1	0.168
5	0.67	52	23	0.46	4.02	554.5	±6.7	725	±150	31	11.13	1.3	0.0635	7	0.786	7.1	0.0898	1.3	0.178	7.1	0.0898	1.3	0.178
4	0.54	112	85	0.78	8.74	555.3	±4.8	547	±140	–2	11.12	0.91	0.0585	6.2	0.725	6.3	0.0899	0.91	0.145	6.3	0.08997	0.91	0.145
6	0.25	99	82	0.86	7.75	560.6	±4.8	566	±90	1	11.007	0.9	0.059	4.1	0.739	4.2	0.0908	0.9	0.212	4.2	0.09085	0.9	0.212
8	0.31	205	159	0.80	16.1	561.8	±3.9	551	±72	–2	10.982	0.73	0.0586	3.3	0.735	3.4	0.0910	0.73	0.217	3.4	0.09106	0.73	0.217
3	0.61	35	17	0.51	2.8	572.3	±8.9	719	±140	26	10.77	1.6	0.0633	6.7	0.811	6.9	0.0928	1.6	0.235	6.9	0.0928	1.6	0.235
9	1.08	1890	1741	0.95	767	2471.9	±5.7	2632.5	±4.2	6	2.1398	0.28	0.1778	0.25	11.457	0.38	0.4673	0.28	0.741	0.38	0.4673	0.28	0.741
10	0.02	584	23	0.04	256	2655.4	±8.4	2721.7	±6	2	1.9619	0.38	0.18765	0.36	13.188	0.53	0.5097	0.38	0.728	0.53	0.5097	0.38	0.728
2	0.01	959	180	0.19	424	2673.6	±7.3	2708.6	±3.7	1	1.9456	0.33	0.18617	0.23	13.193	0.4	0.514	0.33	0.827	0.4	0.514	0.33	0.827

Note. The error constitutes 1σ; the error of standard calibration is 0.31-0.37 %; Pbc and Pb* – total and radiogenic lead; (1) – isotopic ratios are corrected according to the measured ^{204}Pb; *D* – discordance; Rho — correlation coefficient between the determinations of isotopic ages.

© Aleksandr N. Sirotkin, Aleksandr N. Evdokimov, Marina Yu. Burnaeva, Natalya A. Rumyantseva, 2026



This is an open access article under the CC BY 4.0 license

A sample of zircon grains from the greenstone rock of sample 4969-6 comprised 100 grains. Zircon is represented by colourless and light-pink, transparent and translucent angular or irregular fragments, subhedral crystal fragments, and rounded grains; some grains contain inclusions and microfractures. The elongation of zircon grains ranges from 55 to 159 μm. In CL images, zircon exhibits a complex internal structure with clearly expressed oscillatory zoning (e.g., grains 4-10 in Fig.7, *a*).

A concordant U-Pb age of 574.1 ± 4.3 Ma (MSWD = 0.0053) was obtained for nine out of ten grains (Fig.7, *b*, Table 2). For grain 3, an ancient U-Pb age of 1675 ± 18 Ma was recorded. This grain stands out against the background of other dated varieties due to its rounded shape and integrity, whereas the remaining grains are represented by angular fragments (Fig.7, a) and feature a light (near-white) rim in the marginal zone. U content in zircon varies from 113 (analysis point 4 in Fig.7, *a*) to 272 g/t (analysis point 10 in Fig.7, *a*). Th content is more variable, ranging from 65 (analysis point 4 in Fig.7, *a*) to 155 g/t (analysis point 10 in Fig.7, *a*). As in the previously described grains, the lowest U and Th concentrations are found in the light zones, while the highest concentrations occur in the dark zones in CL images. The Th/U ratio ranges from 0.42 to 0.87 (average 0.60), with the maximum value characterising grain 3.

A zircon sample from metandesite sample 4973-1 comprises 85 grains. Zircon is represented by light pink-brown, transparent, prismatic crystal fragments; some grains contain inclusions and/or microfractures. Zircon length ranges from 57 to 223 μm, with an elongation ratio of 2.6-2.7. All zircon grains are crystal fragments; oscillatory zoning can be observed in some of them (e.g., grains 4, 6, 8 in Fig.7, *a*).

A U-Pb age of 558.3 ± 4.3 Ma (MSWD = 0.34) was obtained for seven out of ten grains (Fig.7, *b*, Table 2). Grains 2, 9 and 10, which appear nearly black in CL images (Fig.7, *a*), yielded older ages ranging from 2721.7 ± 6.0 Ma to 2632.5 ± 4.2 Ma. U content varies from 35 to 1890 g/t, Th content – from 17 to 1741 g/t, and the Th/U ratio – from 0.04 to 0.95. The highest U and Th concentrations are characteristic of the oldest, darkest grains in the study set.

Discussion

The data on the study of the sedimentary-volcanic sequence described in the inner regions of the southern part of Oscar II Land (and presented above) allow confident identification of metavolcanic rocks in this area, associated with the Vendian tectono-magmatic activation that occurred here at 574-558 Ma.

Vendian-age complexes have long been known in Spitsbergen. Initially, they were generally described as terrigenous, forming part of the Caledonian basement of the archipelago. Later, a study [1] emerged in which the Vendian complexes of Spitsbergen were interpreted as "platform-like", and the presence of coarse-clastic varieties (tillites) within the terrigenous succession was proposed as evidence of a major tectonic activation. In turn, A.A.Krasilshchikov [10] describes the Vendian complex of the archipelago as carbonate-terrigenous, characterised by fossil assemblages. This provides grounds to assume that during the Vendian, a specific tectonic and physiographic setting existed in the Spitsbergen region. This setting led to a molasse-like appearance of the Vendian formations and was associated with a general uplift of the archipelago's area.

W.B.Harland [20], summarising many years of research on the Vendian deposits in Spitsbergen, suggests that the Vendian sequences in the Oscar II Land area (the St. Jonsfjorden and Comfortlessbreen groups) formed in a rift structure under conditions of alternating glaciation and volcanic epochs. According to the author, the highest intensity of volcanic processes occurred during the accumulation of the upper section in the St. Jonsfjorden Group. However, the authors of the geological map of the southern part of Oscar II Land (scale 1:100,000) [21] identify the volcanic sequence of this area as the Trollheimen and Løvliebreen formations, date them as Mesoproterozoic, and describe a structure where these formations make up the core of a large anticline.

This is an open access article under the CC BY 4.0 license

Thus, the question on the origin and age of the volcanic rocks of the Trollheimen Fm., as well as their place in the overall structure of the region, is fundamental. In a similar structural-facies zone, south of Oscar II Land and in the northern part of WJL, a sedimentary-volcanic sequence of Vendian age – the Chamberlaindalen Series – was described [6]. The geological and petrological framework of this sequence are largely comparable to those of the metavolcanic rocks of the Trollheimen Fm. The zircon ages obtained from rocks of the Trollheimen Fm. allow identifying a new Vendian straton in this part of the archipelago. The rocks of this straton correlate well with the metavolcanic rocks of the Chamberlaindalen Series in terms of age and other features. These include, first of all, the subalkaline and alkaline composition of the Vendian metabasites and their formation under intraplate continental conditions.

The key issue is the relationship between the Vendian volcanic sequence of the Trollheimen Fm. and the previously identified Vendian terrigenous deposits of the Comfortlessbreen Series in the same area, which were characterised paleontologically [22]. In the northern part of WJL, two Vendian-age series – the terrigenous Cap Lyell and the sedimentary-volcanic Chamberlaindalen – occur in the stratigraphic sequence on the basis that tillites of the Cap Lyell Series lack clasts of mafic volcanic rocks that make up the Chamberlaindalen Series sequence [6]. A similar situation is observed in the study area: during mapping of the Comfortlessbreen Series rocks, no clasts of mafic volcanic rocks were described in the metatillites. Data from British geologists [20], who conducted statistical observations of the petrographic composition of clasts in these rocks in the Oscar II Land area, confirm this: among the clasts in the tillites, dolomites, limestones, quartzites, granitoids, and stromatolite-bearing carbonate rocks are described, but mafic volcanic rocks are absent. As another marker, we should cite data on the age of detrital zircons from the Vendian tillites of Nordenskiöld Land (NL, south of Oscar II Land). In the cement of these terrigenous rocks, zircons with ages of 2453-1659, 1503-1383, 1353-1009, and 961-726 Ma were identified. In the same conglomerates, the age of zircons from granite boulders was studied – 2103-1448, 973 ± 10, and 656 ± 5 Ma [32]. It is important to note that in sandstones of the Carboniferous of NL and the Lower Palaeozoic of WJL, detrital zircons with ages in the range 540-510 Ma were identified [32, 33]. Therefore, it can be assumed that the volcanic rocks of the Trollheimen Fm. were formed later than the tillites of the Comfortlessbreen Series and should occur higher in the Vendian sequence.

To clarify the structure of the area, the authors of this paper analysed all available data on rock dip and strike, incorporating data from previous researchers. The obtained result aligns best with the concepts proposed by W.B.Harland [20] and demonstrates the presence of an inset structure in this area, which can be interpreted as a graben. The cross-section (see Fig.2) shows its western shoulder (the eastern flank is truncated by a later structure – the West Spitsbergen graben-like trough).

Conclusion

We obtained absolute age dating of rocks from the Trollheimen Fm. Based on these data, the sequence that W.B.Harland [19, 20] considered as a single coeval straton should be stratified into two units of different ages: the Middle Riphean volcanic-sedimentary Løvliebreen Fm. and the Vendian volcanic Trollheimen Fm.

The presence of the Vendian volcanic rocks in this part of Spitsbergen is identified for the first time, although it was previously predicted [20]. The Vendian in Spitsbergen has long been regarded as a time of activation [1, 3, 10, 34, 35], primarily tectonic [4, 36], as well as magmatic [6, 20]. If tectonic activation is marked by horizons of the Vendian tillites known in all parts of the archipelago [10, 20] and by assemblages of the Timanian mesostructures in the Riphean rocks [4], then the Vendian volcanic rocks are now known from two areas – the northern part of WJL [6] and the southern part of Oscar II Land. Similarities in geological setting, petrological profile, and age data indicate a common formation mechanism for the two complexes. This also provides a sound basis for predicting the discovery of new Vendian volcanic complexes in other parts of the archipelago.

This is an open access article under the CC BY 4.0 license

Data on the metavolcanic rocks of the Trollheimen Fm. demonstrate that the Vendian volcanism in the archipelago is associated with intraplate processes, which were previously described for the volcanic rocks of the Chamberlaindalen Series. The results of studying the petrochemical features of the Trollheimen volcanic formation – the uneven increase in the contents of large-ion lithophile elements and high-field-strength elements relative to heavy rare-earth elements – indicate that the magma originated at great depths, at the level of melting in the upper mantle [37, 38]. The variation of volcanic rocks in terms of alkalinity type, along with the low and reduced contents of compatible elements such as Cr, Ni, Co, etc., points to an anatectic nature of mantle melting in the magma chamber, its relative depth, and evolution over time up to the base of the lower crust. The smooth pattern of light and heavy rare-earth element distribution, together with the prevailing tendency of compositions towards the field of their occurrence in intraplate continental settings, provides grounds to consider these rocks as products of volcanic activity under conditions of continental intraplate rifting.

REFERENCES

1. Barkhatov B.P. The main stages of tectonic development of the Svalbard archipelago. *Vestnik Leningradskogo universiteta*. 1970. N 6. Iss. 1, p. 157-159 (in Russian).
2. Leonov Yu.G. Tectonic nature of the Devonian orogeny. Moscow: Nedra, 1976, p. 192 (in Russian).
3. Turchenko S.I. Pre-Caledonian stage of tectonic development of the Svalbard archipelago folded basement as a basement of an ancient platform. Geologiya i perspektivy rudonosnosti fundamenta drevnikh platform. Leningrad: Nauka, 1987, p. 222-231 (in Russian).
4. Kuznetsov N.B. Svalbard basement: north-eastern prolongation of Scandinavian Caledonides or north-western continuation of Protouralides-Timanides. *Byulleten Moskovskogo obshchestva ispytatelei prirody. Otdel geologicheskii.* 2009. Vol. 84. Iss. 3, p. 23-51 (in Russian).
5. Sirotkin A.N., Evdokimov A.N. Endogenous regimes and evolution of regional metamorphism of folded complexes of the Svalbard archipelago basement (exemplified by the Ny Friesland peninsula). St. Petersburg: VNIIOkeangeologiya im. I.S.Gramberga, 2011, p. 270 (in Russian).
6. Sirotkin A.N., Evdokimov A.N. Vendian age of igneous rocks of the Chamberlain valley area (Northern part of the Wedel Jarlsberg Land, Svalbard Archipelago). *Journal of Mining Institute.* 2022. Vol. 255, p. 419-434. DOI: 10.31897/PMI.2022.20
7. Khain V.E., Filatova N.I. On the prehistory of the modern Arctic Ocean. Geologiya polyarnykh oblastei: Materialy XLII Tektonicheskogo soveshchaniya, 3-6 fevralya 2009, Moskva, Rossiya: v 2 tomakh. Moscow: GEOS, 2009. Vol. 2, p. 260-266 (in Russian).
8. Akbarpuran Haiyati S.A., Gulbin Yu.L., Sirotkin A.N., Gembitskaya I.M. Compositional Evolution of REE- and Ti-Bearing Accessory Minerals in Metamorphic Schists of Atomfjella Series, Western Ny Friesland, Svalbard and Its Petrogenetic Significance. *Geology of Ore Deposits.* 2021. Vol. 63. N 7, p. 634-653. DOI: 10.1134/S1075701521070047
9. Sirotkin A.N., Nikitin D.V. Peculiiarities of geodynamic development of the Devonian Graben at Spitsbergen archipelago. *Journal of Mining Institute.* 2011. Vol. 194, p. 104-111.
10. Krasilshchikov A.A. Stratigraphy and paleotectonics of the Precambrian – Early Paleozoic of Svalbard. Leningrad: Nedra, 1973, p. 120 (in Russian).
11. Turchenko S.I., Tebenkov A.M., Barkhatov D.B., Barmatenkov I.I. Geology and magmatism of the Chamberlain Valley region, Spitsbergen. Geology of Svalbard. Leningrad: Sevmorgeologiya, 1983, p. 38-48 (in Russian).
12. Bjørnerud M. An Upper Proterozoic unconformity in northern Wedel Jarlsberg Land, southwest Spitsbergen: lithostratigraphy and tectonic implications. *Polar Research*. 1990. Vol. 8. N 2, p. 127-139. DOI: 10.3402/polar.v8i2.6809
13. Balašov Yu.A., Peucat J.J., Tebenkov A.M. et al. Rb-Sr whole rock and U-Pb zircon datings of the granitic-gabbroic rocks from the Skålfjellet Subgroup, southwest Spitsbergen. *Polar Research*. 1996. Vol. 15. N 2, p. 167-181. DOI: 10.3402/polar.v15i2.6645
14. Gee D.G., Tebenkov A.M. Two major unconformities beneath the Neoproterozoic Murchisonfjorden Supergroup in the Caledonides of central Nordaustlandet, Svalbard. *Polar Research*. 1996. Vol. 15. N 1, p. 81-91. DOI: 10.3402/polar.v15i1.6638
15. Stratigraphic dictionary of Svalbard. Leningrad: Nedra, 1990, p. 203 (in Russian).
16. Soviet geological research in Svalbard 1962-1992. Extended abstracts of unpublished reports. Ed. by A.A.Krasilščikov. Oslo: Norsk Polarinstitutt, 1996, p. 103.
17. Krasilshchikov A.A., Kovaleva G.A. Precambrian lithostratigraphic complexes of the western coast of Spitsbergen. Geology of Svalbard. Leningrad: Nauchno-issledovatelskii institut geologii Arktiki, 1976, p. 63-70 (in Russian).
18. Hjelle A., Ohta Y., Winsnes T. Hecla Hoek rocks of Oscar II Land and Prins Karls Forland, Svalbard. The geological development of Svalbard during the Precambrian, Lower Palaeozoic, and Devonian: Symposium on Svalbard's geology, 2-5 June 1975, Oslo, Norway. Oslo: Norsk Polarinstitutt, 1979, p. 145-169.
19. Harland W.B., Horsfield W.T., Manby G.M., Morris A.P. An outline pre-Carboniferous stratigraphy of central western Spitsbergen. The geological development of Svalbard during the Precambrian, Lower Palaeozoic, and Devonian: Symposium on Svalbard's geology, 2-5 June 1975, Oslo, Norway. Oslo: Norsk Polarinstitutt, 1979, p. 119-144.
20. Harland W.B., Hambrey M.J., Waddams P. Vendian geology of Svalbard. Oslo: Norsk Polarinstitutt, 1993, p. 150.
21. Geological map of Svalbard. Sheet B8G St. Jonsfjorden. 1:100 000. Oslo: Norsk Polarinstitutt, 2003.

This is an open access article under the CC BY 4.0 license

22. Mikhailova N.S., Turchenko S.I. Late Precambrian microfossils of Svalbard and their stratigraphic significance. *Izvestiya Akademii nauk SSSR. Seriya geologicheskaya*. 1986. N 3, p. 18-25 (in Russian).

23. Raabeh M.E., Zabrodin V.E. Algal problematic of the upper Riphean (stromatolites, oncolites). Moscow: Nauka, 1972, p. 128 (in Russian).

24. Williams I.S. U-Th-Pb Geochronology by Ion Microprobe. Applications of Microanalytical Techniques to Understanding Mineralizing Processes. Society of Economic Geologists, 1998, p. 1-35. DOI: 10.5382/Rev.07.01

25. McDonough W.F., Sun S.-s. The composition of the Earth. *Chemical Geology*. 1995. Vol. 120. Iss. 3-4, p. 223-253. DOI: 10.1016/0009-2541(94)00140-4

26. Whitney D.L., Evans B.W. Abbreviations for names of rock-forming minerals. *American Mineralogist*. 2010. Vol. 95. N 1, p. 185-187. DOI: 10.2138/am.2010.3371

27. Middlemost E.A.K. The basalt clan. *Earth-Science Reviews.* 1975. Vol. 11. Iss. 4, p. 337-364. DOI: 10.1016/0012-8252(75)90039-2

28. Mullen E.D. $MnO/TiO_2/P_2O_5$: a minor element discriminant for basaltic rocks of oceanic environments and its implications for petrogenesis. *Earth and Planetary Science Letters*. 1983. Vol. 62. Iss. 1, p. 53-62. DOI: 10.1016/0012-821X(83)90070-5

29. Pierce A.B., Bell J.M., Owen B.D., Doige C.E. Availability of phytate phosphorus to the growing pig receiving isonitrogenous diets based on wheat at corn. *Canadian Journal of Animal Science*. 1977. Vol. 57. N 3, p. 573-583. DOI: 10.4141/cjas77-074

30. Meschede M. A method of discriminating between different types of mid-ocean ridge basalts and continental tholeiites with the Nb-1bZr-1bY diagram. *Chemical Geology*. 1986. Vol. 56. Iss. 3-4, p. 207-218. DOI: 10.1016/0009-2541(86)90004-5

31. Wood D.A. The application of a Thsingle bondHfsingle bondTa diagram to problems of tectonomagmatic classification and to establishing the nature of crustal contamination of basaltic lavas of the British Tertiary Volcanic Province. *Earth and Planetary Science Letters*. 1980. Vol. 50. Iss. 1, p. 11-30. DOI: 10.1016/0012-821X(80)90116-8

32. Sirotkin A.N., Marin Yu.B., Kuznetsov N.B. et al. The Age of Spitsbergen Basement Consolidation: U-Pb Dating of Detrital Zircons from the Upper Precambrian and Lower Carboniferous Clastic Rocks of the Northwestern Part of Nordenskiöld Land. *Doklady Earth Sciences.* 2017. Vol. 477. Part 1, p. 1282-1286. DOI: 10.1134/S1028334X17110253

33. Kosteva N.N., Kuznetsov N.B., Tebenkov A.M., Romanyuk T.V. First Results of the U-Pb Isotopic (LA-ICP-MS) Dating of Detrital Zircons from the Lower Paleozoic of Spitsbergen. *Doklady Earth Sciences.* 2014. Vol. 455. Part 1, p. 259-265. DOI: 10.1134/S1028334X1403026X

34. Sirotkin A.N., Evdokimov A.N. New data on U-Pb dating of basic and ultrabasic metamorphosed intrusions in the north Ny-Friesland Peninsula (Spitsbergen). *Regional Geology and Metallogeny.* 2020. N 81, p. 45-59 (in Russian).

35. Gulbin Yu.L., Akbarpuran Khaiyati S.A., Sirotkin A.N. Mineral composition and thermobarometry of metamorphic rocks of Western Ny Friesland, Svalbard. *Journal of Mining Institute.* 2023. Vol. 263, p. 657-673.

36. Kuznetsov N.B. Neoproterozoic – Early Paleozoic tectonic history of Western Arctic (regional geological and paleotectonic aspects). Structure and Evolution of the Lithosphere. Moscow: Paulsen, 2010, p. 525-569 (in Russian).

37. Ivanov A.V. Intracontinental basaltic magmatism (exemplified by the Mesozoic and Cenozoic of Siberia): Avtoref. dis. … d-ra geol.-mineral. nauk. Irkutsk: Institut zemnoi kory Sibirskogo otdeleniya RAN, 2011, p. 30 (in Russian).

38. Akbarpuran Haiyatia S.A., Gulbin Yu.L., Borisovskiy S.E. Age of monazite from metapelitic schists of Atomfjella and Mossel series, Western Ny Friesland, Spitsbergen according to the CHIME method. *Vestnik of Geosciences.* 2021. N 10 (322), p. 16-24 (in Russian). DOI: 10.19110/geov.2021.10.2

***Authors*: Aleksandr N. Sirotkin,** *Doctor of Geological and Mineralogical Sciences, Head of Sector* (*VNIIOkeangeologia, Saint Petersburg, Russia*), *https://orcid.org/0000-0003-2433-3953*, **Aleksandr N. Evdokimov,** *Doctor of Geological and Mineralogical Sciences, Professor* (*Empress Catherine II Saint Petersburg Mining University, Saint Petersburg, Russia*), *Evdokimov_AN@pers.spmi.ru*, *https://orcid.org/0000-0002-8121-0426*, **Marina Yu. Burnaeva,** *Candidate of Geological and Mineralogical Sciences, Researcher* (*VNIIOkeangeologia, Saint Petersburg, Russia*), *https://orcid.org/0009-0008-5015-5023*, **Natalya A. Rumyantseva,** *Candidate of Geological and Mineralogical Sciences, Leading Engineer* (*VNIIOkeangeologia, Saint Petersburg, Russia*), *https://orcid.org/0000-0002-1173-4101*.

The authors declare no conflict of interests.

This is an open access article under the CC BY 4.0 license